

# 1 **Finite element model of salami ripening process and successive storage in package**

2

3 Chiara Cevoli<sup>a\*</sup>, Angelo Fabbri<sup>a</sup>, Giulia Tabanelli<sup>b</sup>, Chiara Montanari<sup>b</sup>, Fausto Gardini<sup>ab</sup>, Rosalba  
4 Lanciotti<sup>ab</sup>, Adriano Guarnieri<sup>a</sup>

5

6 <sup>a</sup>*Department of Agricultural and Food Sciences, University of Bologna, P.zza Goidanich 60,47521, Cesena (FC), Italy;*

7 <sup>b</sup>*CIRI-Interdepartmental Centre of Agri-Food Industrial Research, University of Bologna, P.zza Goidanich 60, 47521,*

8 *Cesena (FC), Italy; \*Corresponding author: chiara.cevoli3@unibo.it*

9

## 10 **Abstract**

11 Salami are typical European dry fermented sausages manufactured mainly with pork meats. Water  
12 loss is a crucial aspect of industrial ripening process because it is responsible for the lowering of  
13 water activity, which determines limitations to successive conservation.

14 This paper describes two parametric numerical models developed to study the moisture diffusion  
15 physics, during ripening and storage in package. Mass transfer equations inside the sausage volume  
16 were numerically solved using a finite element technique. A first model describes diffusion  
17 phenomena occurring inside the salami and the exchange phenomena involving the surface of the  
18 product and the industrial environment, while a second one describes also the evaporation and  
19 condensation phenomena occurring between the salami surface and the atmosphere inside the  
20 packaging. The models were experimentally validated showing a good agreement with observed  
21 data.

22 The numerical models allowed to study the water transfer inside of dry fermented sausages with a  
23 detail unreachable by any experimental technique. In addition the models could be used to find the  
24 best conditions for ripening, packaging and distribution.

25

26 **Keywords:** numerical simulation, models, mass transfer, sausage.

27

## 28 **1. Introduction**

29 Dry fermented sausages are the result of a fermentation process and a ripening period during which  
30 the products reach the desired characteristics. From several centuries, different kind of dry  
31 fermented sausages have been produced in the Mediterranean area (Toldrá et al., 2007; Zeuthen,  
32 1995; Ordóñez et al 1999). The wide variety of dry fermented sausages is a consequence of  
33 variations in formulation, raw material, manufacturing and ripening processes which come from the  
34 traditional habits of different countries and regions (Zanardi et al., 2010). Often fermented sausages  
35 get different names according to geographic origin (Toldrá, 2006). In particular, salami are typical

36 European dry fermented sausages manufactured mainly with pork, but also with bovine, ovine and  
37 equine meats, with the addition of salt, curing agents (nitrate and nitrite), spices, and sometimes  
38 herbs and/or other ingredients (Feiner, 2006).

39 The primary European countries producing salami are Germany, Italy, Spain, France and Hungary,  
40 with a production of several hundred-millions kg per year, and ripening and storage periods play an  
41 important role on the final characteristics of these fermented sausages (Bertolini et al., 2006). In  
42 particular, in the dry fermented sausages industry, ripening is considered one of the most important  
43 stages of the integrated supply chain needed to ensure that end products have the final requirements  
44 in terms of quality and safety standards (Grassi and Montanari, 2005). In fact, the ripening stage  
45 influences over the main physical, chemical and microbiological transformations that take place in  
46 salami after manufacturing.

47 A large number of studies regarding the influence of ripening conditions on the microbiological,  
48 physical and chemical properties of dry fermented sausages are available (Baldini et al., 2000;  
49 Campbell-Platt and Cook, 1995; Zanardi et al., 2010; Tabanelli et al 2012; Tabanelli et al. 2013).  
50 All these researches show that the final quality and safety standards achieved by the sausage  
51 manufacturing process can be considered to be strictly dependent from the conditions under which  
52 ripening stage is designed and carried out (Rizzi, 2003).

53 The most important mass transport phenomenon occurring inside the matrix during ripening is the  
54 water transfer. Many theoretically and experimentally studies about transfer of water and solutes  
55 through meat and meat products matrices are reported in literature (Costa-Corredor et al., 2009;  
56 Graiver et al., 2006; Hansen et al., 2008; Sabadini et al., 1998; Unal et al., 2004). Water loss is a  
57 crucial aspect of ripening because it is responsible for the lowering of water activity ( $a_w$ ), which  
58 determines limitations to the growth of many spoilage and pathogenic microorganisms. In addition,  
59 the water loss has to be as uniform as possible to avoid the formation of moisture gradients in the  
60 sausages causing the case hardening which is negative for the textural properties and also for the  
61 safety of the final products. Water loss can be modulated during ripening by controlling the  
62 temperature of the ripening chambers and their relative humidity (Feiner, 2006).

63 As reported in many specific reviews, the recent progress in computing efficiency coupled with  
64 reduced costs of codes has set out the numerical simulation as a powerful tool to study many food  
65 processes with the aim of providing effective and efficient plant design or operating solutions (Scott  
66 and Richardson, 1997; Xia and Sun, 2002; Wang and Sun, 2003; Norton and Sun, 2006; Smale et  
67 al., 2006; Verboven et al., 2006; Mirade, 2008). In this regard, the numerical simulation was used to  
68 study the mass transfer in various foods during drying, baking, freezing and ripening (Mirade, 2008;  
69 Sakin et al., 2007; Lemus-Mondaca et al., 2013; Floury et al., 2008).

70 As concerning the salami ripening, Rizzi (2003) developed a parametric model for the fluid  
71 dynamic simulation of ascending flow ripening chambers as a function of operational conditions.  
72 The model was experimentally validated comparing measured and simulated air velocity modules.  
73 Grassi and Montanari (2005) developed a parametric model very similar to that of Rizzi (2003), but  
74 in addition, the authors built a sausage drying model that computes mass and heat exchange  
75 between sausage and the air flows. However, the model has not been experimentally validated.  
76 The aim of this research was to develop two parametric numerical models, concerning the moisture  
77 diffusion physics, describing salami ripening and storage. Mass transfer equations inside the  
78 sausage volume were numerically solved using a finite element technique. A first model describes  
79 diffusion phenomena occurring inside the salami and the exchange phenomena involving the  
80 surface of the product and the environment, while a second one describes also the evaporation and  
81 condensation phenomena occurring between the salami surface and the atmosphere after the whole  
82 sausage packaging. The models was experimentally validated, comparing the numerical outputs of  
83 the simulations with experimental data. In addition, the models could be used to find the best  
84 conditions at which whole fermented sausages should be packaged for distribution.

85

## 86 **2.Materials and methods**

### 87 *2.1 Ripening model*

88 Commercial computational multiphysics codes are available nowadays, allowing an exceedingly  
89 flexible simultaneous numerical solution of the energy, mass and moment equation (Scott and  
90 Richardson, 1997) and are extensively adopted in the food engineering field (Xia and Sun, 2002;  
91 Wang and Sun, 2003; Norton and Sun, 2006; Fabbri et al., 2011).

92 The equations of mass transfer inside and on the salami surface were solved using Comsol  
93 Multiphysics 4.3 (COMSOL Inc., Burlington, MA, USA), a commercial partial differential  
94 equations solver, based on finite element technique. During ripening, the moisture diffuses from the  
95 inside, towards the salami surface and about half of the initial water content is lost through  
96 evaporation. To simulate moisture transfer inside of product, salami material was treated as  
97 homogeneous and isotropic, initial moisture was set uniform and salami volume was considered  
98 constant.

99 In order to limit the computation time, an one-dimensional model was built because the salami  
100 geometry is axisymmetric and it was considered an indefinite length salami. Subsequently, with a  
101 simple geometric operation, a 2D model can be visualized. The geometry dimensions reflect the real  
102 ones of the salami considered, in particular a simple radius ( $r$ : 25 mm) between the longitudinal axis  
103 and the external cylindrical surface was considered.

104 The moisture transfer is governed by Fick's law:

$$105 \quad \frac{\partial C}{\partial t} = D_{H_2O} (\nabla^2 C) \quad (1)$$

106 where  $C$  is calculated moisture concentration ( $\text{mol m}^{-3}$ ) at time  $t$ .

107 Mass diffusivity ( $D_{H_2O}$ ) through the involved material was found in literature (Simal et al., 2003;  
108 Trujillo et al., 2007).

109 Initial moisture concentration ( $C_{Rin}$ ) was considered constant in space and defined as following:

$$110 \quad C_{Rin} = \left( \frac{X_{Rin} \cdot \rho_s}{PM_{H_2O}} \right) \quad (2)$$

111 where  $X_{Rin}$  is the initial moisture content on dry basis (experimentally determined:  $1.2 \text{ kg kg}^{-1}$ ),  $\rho_s$   
112 the dried salami density (experimentally determined:  $600 \text{ kg m}^{-3}$ ), while  $PM_{H_2O}$  the water molecular  
113 weight ( $0.018 \text{ kg mol}^{-1}$ );

114 A flux condition was imposed on the interface between salami surface and air:

$$115 \quad N_R = k_t (C_{bound} - C) \quad (3)$$

116 being  $N_R$  ( $\text{mol m}^{-2} \text{ s}^{-1}$ ) the water flux,  $k_t$  ( $\text{m s}^{-1}$ ) the mass transfer coefficient and  $C_{bound}$  the moisture  
117 concentration of salami at equilibrium.

118 Mass transfer coefficient can vary within very broad limits, without problems of physical model  
119 fidelity: convergence could be compromised for high values, while for small values an artificial  
120 resistance to the moisture passage could be introduced. A value must therefore be determined  
121 empirically by choosing a level slightly lower than that which causes convergence problems (in our  
122 case  $k_t$ :  $1\text{E-}6 \text{ m s}^{-1}$ ).

123 Moisture concentration of salami at equilibrium was defined by following equation:

$$124 \quad C_{bound} = \left( \frac{X_{bound} \cdot \rho_s}{PM_{H_2O}} \right) \quad (4)$$

125 where  $X_{bound}$  is the moisture content on dry basis at equilibrium. This value was determined by using  
126 the Oswin law:

$$127 \quad X_{bound} = A \left[ \frac{a_w}{(1 - a_w)} \right]^B \quad (5)$$

128 being  $a_w$  value equal to that of relative humidity of the ripening room by definition. A (0.4287) and  
129 B (0.2397) parameters were determined by fitting the experimental data of water activity vs  
130 moisture content, measured during the ripening, with the Oswin law.

131 Model was validated by comparing water activity and water concentration, numerically and  
 132 experimentally determined. For the experimental determination a Milano type dry fermented salami  
 133 made with pork shoulder (72% w/w) and streaky bacon (28% w/w), NaCl (2.6% w/w), dextrose  
 134 (0.30% w/w), KNO<sub>3</sub> (0.015% w/w), NaNO<sub>2</sub> (0.010% w/w), wine (1% w/w) and spices (white  
 135 pepper powder and black pepper whole grain, 0.12% w/w) was used (Tabanelli et al. 2013).  
 136 Salami had a length of about 200 mm, a diameter of about 50 mm and an initial mean weight of  
 137 about 430 g. The drying conditions were the following: 48 h at 23 °C and relative humidity (RH) of  
 138 70%, 48 h at 21 °C and RH of 80%, 24 h at 19 °C and RH of 83%, and finally 24 h at 17 °C and RH  
 139 of 86%. Then salami were transferred to the ripening chamber at 15 °C and RH of about 80%.  
 140 During the ripening, the weight loss was monitored and  $a_w$  was measured by using an Aqualab  
 141 CX3-TE (Labo-Scientifica, Parma, Italy). All the measures were done in triplicate at different days  
 142 of ripening.

143

## 144 2.2 Storage model

145 Sausages were taken off from ripening chamber at different mean  $a_w$  values, packaged in plastic  
 146 film and stored at room temperature. The physical and biochemical activities inside the sausages are  
 147 not stopped at this phase and proceed with a rate depending on several factors, the main of which is  
 148 temperature. The main goal of plastic package is to avoid further water loss that can cause  
 149 economic damages. During storage exchange phenomena (evaporation and condensation) between  
 150 product and air within packaging, as function of temperature, were possible.

151 For the storage model, the same software, geometry and physical parameters of the salami ( $D_{H_2O}$ ) of  
 152 ripening model were used. Salami material was considered homogeneous and isotropic while its  
 153 volume was considered constant. Also the total water mass of the salami/air packaging system was  
 154 defined as constant, as the packaging material were a perfect barrier for air and water. Even in this  
 155 case, the phenomenon of mass transfer inside solid phase is governed by Fick's law.

156 Initial moisture concentration ( $C_{Sin}$ ) was defined as following:

$$157 \quad C_{Sin} = \left( \frac{X_{Sin} \cdot \rho_s}{PM_{H_2O}} \right) \quad (6)$$

158 where  $X_{Sin}$  is the initial moisture content on dry basis determined by previous model as function of  
 159 coordinate  $r$ .

160 A flux condition ( $N_s$  [mol m<sup>-2</sup> s<sup>-1</sup>]) on the interface between the surface of the salami and the air of  
 161 the packaging, as function of the partial pressure, was imposed (Mujumdar and Menon, 1995):

162 
$$N_S = k_t \left( \frac{\rho_{air}}{PM_{H_2O}} \right) \cdot \left( \frac{PM_{H_2O}}{PM_{air}} \right) \cdot \left( \frac{\varphi_{air} \cdot P_{airSat}}{P_{atm} - \varphi_{air} \cdot P_{airSat}} - \frac{a_{wair} \cdot P_{airSat}}{P_{atm} - a_{wair} \cdot P_{airSat}} \right) \quad (7)$$

163 where:

164 
$$\rho_{air} = \left( \frac{P_{atm} \cdot PM_{air}}{RT} \right) : \text{air density [kg m}^{-3}\text{]}; \quad (8)$$

165  $P_{atm}$ : atmospheric pressure [1E+5Pa];

166  $PM_{air}$ : air molecular weight [28.84 g mol<sup>-1</sup>];

167  $R$ : gas constant [8.314 J K<sup>-1</sup> mol<sup>-1</sup>];

168  $T$ : temperature, sinusoidally varying on a 24 h basis [K];

169 
$$\varphi_{air} = \frac{P_{air}}{P_{airSat}} : \text{relative humidity of air/water vapour mixture}; \quad (9)$$

170 
$$P_{air} = \frac{M_{H_2Oair} \cdot RT}{PM_{H_2O} \cdot V_{air}} : \text{partial pressure of water vapour [Pa]}; \quad (10)$$

171 
$$M_{H_2Oair} = (M_{H_2OTot} - M_{H_2OS} - M_{H_2OLq}) : \text{water mass in the headspace calculated considering} \quad (11)$$

172 mass conservation equation [kg];

173 
$$M_{H_2OTot} = M_s \cdot X_{Sin} : \text{total water mass in the system [kg]}; \quad (12)$$

174  $M_s$ : mass of dry salami [0.280 kg];

175 
$$M_{H_2OS} = (\bar{\rho}_{H_2OS} \cdot V_s) : \text{water mass in salami [kg]}; \quad (13)$$

176 
$$\bar{\rho}_{H_2OS} = \bar{C} \cdot PM_{H_2O} : \text{mean water density [kg m}^{-3}\text{]}; \quad (14)$$

177  $\bar{C}$ : space average concentration [mol m<sup>-3</sup>]

178 
$$\frac{dM_{H_2OLq}}{dt} = F_c - F_e : \text{water mass conservation equation as function of evaporation and} \quad (15)$$

179 condensation phenomena [kg];

180 
$$F_c = K_c \cdot (\varphi_{air} - 1) \cdot \left( \frac{M_{H_2Oair}}{M_{H_2OTot}} \right) \cdot \bar{A} : \text{mass flow of condensing water (always positive but} \quad (16)$$

181 nonzero only for saturated or oversaturated air) [kg s<sup>-1</sup>];

182  $F_e = K_e \cdot (1 - \varphi_{air}) \cdot \left( \frac{M_{H_2OLq}}{M_{H_2OTot}} \right) \cdot \bar{A}$ : mass flow of evaporating water (always positive but

183 nonzero only for unsaturated air) [kg s<sup>-1</sup>]; (17)

184  $\bar{A} = L \pi \cdot (r + r_p)$ : mean exchange area [m<sup>2</sup>]; (18)

185  $L$ : salami length [200 mm];

186  $r_p$ : packaging salami radius [30 mm];

187  $K_c$ : condensation parameter [kg s<sup>-1</sup> m<sup>-2</sup>];

188  $K_e$ : evaporation parameter [kg s<sup>-1</sup> m<sup>-2</sup>];

189  $V_{air}$ : headspace volume [m<sup>3</sup>];

190  $P_{airSat} = \left( 10^{\left( \frac{8.07131 - \frac{1730.63}{233.426 + T}}{760} \right)} \cdot \frac{P_{atm}}{760} \right)$ : saturation pressure of water vapour in air as function of

191 temperature (August-Antoine, 1888) [Pa]; (19)

192  $a_{wair} = \left( \frac{\left( \frac{X_s}{A} \right)^{\left( \frac{1}{B} \right)}}{1 - \left( \frac{X_s}{A} \right)^{\left( \frac{1}{B} \right)}} \right)$ : relative humidity of air near to salami calculated by using Oswin law;

193 (20)

194  $X_{s=} \left( \frac{\bar{C}_c \cdot PM_{H_2O}}{\rho_s} \right)$ : dry basis moisture content on the salami surface [kg kg<sup>-1</sup>]; (21)

195  $\bar{C}_c$ : mean water concentration determined on the exchange surface [mol m<sup>-3</sup>].

196 Model was validated by comparing water activity and dry basis moisture content, numerically and  
 197 experimentally determined in triplicate. For the experimental determination salami ripened for 28  
 198 days at 80% of RH and 15°C (the same type used to validate the ripening model), were packaged in  
 199 a Flexible OPA/PE laminated plastic film (O<sub>2</sub> transmission: 28±1.4 cm<sup>3</sup>/m<sup>2</sup>/24 h/atm and CO<sub>2</sub>  
 200 transmission: 150±7.5 cm<sup>3</sup>/m<sup>2</sup>/24 h/atm) and stored at room temperature (daytime: about 30°C and  
 201 night: about 20°C) for 60 days (Tabanelli et al. 2013).

202

### 203 3. Results

#### 204 3.1 Ripening model

205 To validate the ripening model, only fermented sausages after 28 days of ripening were considered.  
206 In particular, experimental and calculated values of mean water concentration (figure 1) and  $a_w$   
207 (figure 2) were compared.

208 The experimental data of mean water concentration were defined by starting from the weight loss  
209 (%) at 0, 3, 5, 8, 11, 14, 18, 23, and 28 days of ripening. In this case the agreement between  
210 simulated and experimental values was represented by a determination coefficient  $R^2$  of 0.923  
211 ( $p < 0.05$ ). Mean difference between calculated and experimental data is of 4.69% with a minimum  
212 and maximum value of 0.403 and 7.04%, respectively. Calculated data were higher, except for 23  
213 and 28 days of ripening.

214 The  $a_w$  was measured in triplicate at 0, 11, 18, 23, and 28 days of ripening. The agreement between  
215 simulated and experimental values is represented by a determination coefficient  $R^2$  of 0.994  
216 ( $p < 0.05$ ). In this case mean difference between calculated and experimental data is of 0.85% with a  
217 minimum and maximum value of 0.34 and 1.17%, respectively.

218 Both for water concentration to the  $a_w$ , simulated and experimental data were in good agreement.  
219 This result shows that the numerical model was able to reproduce the mass transfer phenomenon  
220 inside of salami.

221 Simulated moisture concentration and relative dry basis moisture content and  $a_w$  inside of salami  
222 after 28 days of ripening is reported in figure 3 (under the same ripening condition used for the  
223 model validation). It can be seen that the moisture was not uniformly placed (Figure 3a), and a  
224 considerable difference between internal (about  $16500 \text{ mol m}^{-3}$ ) and external (about  $26300 \text{ mol m}^{-3}$ )  
225 zone is shown. For the producers, the presence of this gradient can be very critical. In fact, when its  
226 entity is not strictly controlled, the formation of case hardening can take place. This sausage defect  
227 is dependent on the formation of a dry superficial layer due to a too fast removal of water. This  
228 layer forms a barrier which is harder and less permeable than the inner part of the product and  
229 opposes to further water removal. Consequently, water concentration remains high and not uniform  
230 inside (Ruiz-Ramírez et al. 2005), increasing the risks of unwanted microbial growth of both  
231 spoilage and pathogenic species. For this reason, in the fermented sausages the water loss is  
232 regulated through the rigorous control of temperature and relative humidity in the ripening  
233 chambers and also through the growth of moulds in the outer side of casing. This risk is more  
234 evident taking into consideration the  $a_w$  value reported in Figure 3b. These data evidence a thin  
235 layer immediately below the casing in which the  $a_w$  is considerably lower, with the possibility of  
236 crust formation.

237 Also Baldini et al. (2000) found this lack of uniformity in water concentration inside sausages and  
238 reported that in different type of salami, at the end of ripening stages, the drying is much more



239 marked in the external fractions and considerably lower in the internal ones. In particular for salami  
240 characterized by a diameter of about 50-60 mm, an initial moisture content of about 58% and a  
241 ripening time of 28 days (similar conditions to those used in this study), the authors showed that the  
242 final percentages of moistures (internal fraction about 43%, external fraction about 33%) are similar  
243 to those determined by the model (internal fraction about 44%, external fraction about 34%).

244 The variation in water quantity in the internal and external zone during the ripening depends on  
245 salami size. In this study, to evaluate the size effect on the mass transfer, the final water  
246 concentrations (after 28 days of ripening) as a function of radius dimension and position inside of  
247 salami, are reported in Figure 4. It can be seen that the salami size significantly affects the mass  
248 transfer. In fact, doubling the salami radius (from 20 to 40 mm), the final water concentration in the  
249 central zone (radius from 0 to 10 mm) increases of 65% (from 20918 to 34611 mol m<sup>-3</sup>). This aspect  
250 highlights that the assessment of size is an important aspect for the ripening stage.

251 Considering that the variation in water quantity inside of salami should be also connected to the  
252 ripening condition (temperature, RH), mean moisture contents on dry basis as function of RH (75,  
253 80 and 85%) and days of ripening are reported in figure 5. For the first six days the curves were  
254 overlapped because the drying conditions were maintained the same (48 h RH of 70%, 48 h RH of  
255 80%, 24 h RH of 83%, and finally 24 h at RH of 86%). Real ripening time starts after 6 days. It can  
256 be seen that after 28 days, the moisture content on dry basis increased of 5.24% (from 0.642 to  
257 0.675 kg kg<sup>-1</sup>), passing from 75 to 80% of RH and of 6.19% (from 0.675 to 0.717 kg kg<sup>-1</sup>), passing  
258 from 80 to 85% of RH. Also in this case, similar results are reported by Baldini et al. (2000). In  
259 particular for salami characterized by a diameter of about 50-60 mm, and ripened for 28 days, the  
260 authors showed an increase of about 6.42% of moisture on dry basis, passing from 0.82 to 0.87% of  
261 RH (step of 5%).

262

### 263 *3.2 Storage model*

264

265 To validate the storage model, experimental and calculated values of water activity and dry basis  
266 moisture content determined after 60 days at room temperature (daytime: about 30°C and night:  
267 about 20°C) were compared.

268 Experimentally, moisture content changes were not observed. However, some minor variations in  
269 the mean  $a_w$  values were recorded during storage and the values further decreased by about 0.01  
270 units. According to the model a small decrease of mean  $a_w$  (passing from 0.8689 to 0.8691) and dry  
271 basis moisture content were observed (passing from 0.6735 to 0.6738 kg kg<sup>-1</sup>).

272 Moisture content as function of days of storage and position inside of salami is reported in figure 6.  
273 Considering the minimal loss of water, it is possible to confirm that the packaging prevents further  
274 dehydration of the product. Globally, salami water do not diffuses outside but tends to internally  
275 redistribute and equilibrate water content. The moisture content inside of salami was uniformly  
276 placed only after about 35 days of storage.

277 Mass changes of water in air (headspace of the package), inside of salami and liquid (available for  
278 evaporation) during storage, are shown in figure 7. According to what written above, it can be seen  
279 that salami water mass slightly decreases during the storage. However, this reduction causes a liquid  
280 water increase during about the first ten days of storage. In fact, the water moves from salami to  
281 headspace until the air is saturated. The air saturation level depends on the temperature that varying  
282 produces condensation and evaporation phenomena on the salami surface causing a very small  
283 oscillation of moisture content during storage. As the temperature decrease, the headspace air  
284 became over-saturated releasing some water. Particularly, when temperature increase ( $\leq 30^{\circ}\text{C}$ ),  
285 water evaporate and moisture content of salami slightly decrease, while when temperature decrease  
286 ( $\geq 20^{\circ}\text{C}$ ), water condense and moisture content of salami increase.

287 In the figure 8, it can be seen that the moisture variation, as an example for a salami storage for 20  
288 days , affects about the outer 4 mm of salami radius. The black lines concern the temperature  
289 decrease, while the grey line are relative to the temperature increase. These continuous variations of  
290 moisture content and consequent liquid film deposition, in the first few millimeters closer to the  
291 surface, could affect the texture of external zone of salami. In addition, variation of  $a_w$  in microareas  
292 of the surface of sausages, even if minimum, can create conditions more favorable to a intermittent  
293 activity of microbial species whose presence is negative for sausage overall quality. In agreement  
294 with this hypothesis, salami used for the storage model validation showed a softening of the first  
295 millimetres of product that could significantly compromise the product quality.

296

## 297 **Conclusions**

298 The numerical models allowed to study the mass transfer of the water inside of dry fermented  
299 sausages, during the ripening and storage phases, with a detail unreachable by any experimental  
300 technique. The results of the models, in integral form, were in good agreement with those  
301 experimentally observed.

302 The model clarifies the mass diffusion mechanism that moves moisture from the inner part of  
303 salami to its surface: whatever are the environmental conditions, the moisture in the headspace  
304 reaches an equilibrium with the moisture inside the meat. During the conservation the moisture  
305 concentration tends, by mass diffusion, to become uniform in space, flowing from the centre to the

306 periphery. As the environmental temperature decreases, the head-space air becomes over-saturated  
307 releasing some water. This liquid state water drops on the salami surface and can compromise the  
308 conservation conditions in relation to the packaged sausage  $a_w$ . During the conservation time, every  
309 temperature oscillation activates this water movement mechanism.

310 Ultimately, the numerical model represents a powerful and versatile industrial instrument and, being  
311 parametric, wide spanning data input regarding time, ripening and storage temperatures, size and  
312 type of sausage, etc. can be tested.

313

## 314 **References**

315

316 Baldini P., Cantoni E., Colla F., Diaferia C., Gabba L., Spotti E., Marchelli R., Dossena A., Virgili  
317 E., Sforza S., Tenca P., Mangia A., Jordano R., Lopez M.C., Medina L., Coudurier S., Oddou S.,  
318 Solignat G. (2000). Dry sausages ripening: influence of thermohygro-metric conditions on  
319 microbiological, chemical and physico-chemical characteristics, *Food Research International*, 33,  
320 161-170.

321

322 Bertolini M., Ferretti G., Grassi A., Montanari R. (2006). Seasoning process design optimization for  
323 an ascending flow ripening chamber. *Journal of Food Engineering*, 77, 529-538.

324

325 Campbell-Platt G., Cook P.E. (1995). Fermented meats. Glasgow: Blackie Academic and  
326 Professional.

327

328 Costa-Corredor A., Pakowski Z., Lenczewski T., Gou P. (2010). Simulation of simultaneous water  
329 and salt diffusion in dry fermented sausages by the Stefan–Maxwell equation. *Journal of Food*  
330 *Engineering*, 97, 311-318.

331

332 Fabbri A., Cevoli C., Silaghi F.A., Guarnieri A. (2011). Numerical simulation of physical system in  
333 agri-food engineering. *Journal of Agricultural Engineering*. 4, 1-7.

334

335 Feiner, G. (2006). Meat products handbook: Practical science and technology. Chapter 16, Raw  
336 Fermented Salami, 314-375. Woodhead Publishing Limited, Cambridge LK.

337

338 Flourey J., Le Bail A., Pham Q.T. (2008). A three-dimensional numerical simulation of the osmotic  
339 dehydration of mango and effect of freezing on the mass transfer rates. *Journal of Food*  
340 *Engineering*, 85, 1-11.

341

342 Graiver N., Pinotti A., Califano A., Zaritzky N. (2006). Diffusion of sodium chloride in pork tissue.  
343 *Journal of Food Engineering*, 77, 910-918.

344

345 Grassi A., Montanari R. (2005). Simulation of the thermodynamic patterns in an ascending flow  
346 ripening chamber. *Journal of Food Engineering*, 68, 13-123.

347

348 Hansen C.L., van der Berg F., Ringgaard S., Stodkilde-Jorgensen H., Karlsson A.H. (2008).  
349 Diffusion of NaCl in meat studied by <sup>1</sup>H and <sup>23</sup>Na magnetic resonance imaging. *Meat Science*, 80,  
350 851–856.

351

352 Lemus-Mondaca R.A., Zambra C.E., Vega-Gálvez A., Moraga N.O. (2013). Coupled 3D heat and  
353 mass transfer model for numerical analysis of drying process in papaya slices. *Journal of Food*  
354 *Engineering*, 116, 109-117.

355

356 Mirade P.S. (2008). Computational fluid dynamics (CFD) modelling applied to the ripening of  
357 fermented food products: Basics and advances. *Trends in Food Science & Technology*, 19, 472-481.

358

359 Mujumdar A.S., Menon A.S., (1995). Drying of Solids, pp. 1-46, in A.S. Mujumdar (Ed.)  
360 *Handbook of Industrial Drying*, 2nd Edition, Marcel Dekker, New York.

361

362 Norton T., Sun D.W. (2006). Computational fluid dynamics (CFD) e an effective and efficient  
363 design and analysis tool for the food industry: a review. *Trends in Food Science & Technology*, 17,  
364 600-620.

365

366 Ordóñez J. A., Hierro E. M., Bruna J. M., de la Hoz L. (1999). Changes in the components of dry-  
367 fermented sausages during ripening. *Critical Reviews in Food Science and Nutrition*, 39, 329-367.

368

369 Ruiz-Ramirez J., Serra X., Arnau J., Gou P. (2005) Profiles of water content, water activity and  
370 texture in crusted dry-cured loin and in non-crusted dry cured loin. *Meat Science*, 69, 519-525.

371

372 Rizzi A. (2003). Development of a numerical model for the fluid dynamic simulation of an  
373 ascending flow ripening chamber. *Journal of Food Engineering*, 58, 151–171.

374

375 Sabadini E., Carvalho B.C., do A. Sobral P.J., Hubinger M.D. (1998). Mass transfer and diffusion  
376 coefficient determination in the wet and dry salting of meat. *Drying Technology*, 16, 2095–2115.

377

378 Sakin M., Kaymak-Ertekin F., Ilicali C. (2007). Simultaneous heat and mass transfer simulation  
379 applied to convective oven cup cake baking. *Journal of Food Engineering*, 83, 463–474.

380

381 Scott G., Richardson P. (1997). The application of computational fluid dynamics in the food  
382 industry. *Trends in Food Science & Technology*, 8, 119-124.

383

384 Simal, S., Femenia, A., Garcia-Pascual, P., Rossell, C. (2003). Simulation of the drying curves of a  
385 meat-based product: effect of the external resistance to mass transfer. *Journal of Food Engineering*,  
386 58, 193-199.

387

388 Smale N. J., Moureh J., Cortella G. (2006). A review of numerical models of airflow in refrigerated  
389 food applications. *International Journal of Refrigeration*, 29, 911-930.

390

391 Tabanelli G., Coloretti F., Chiavari C., Grazia L., Lanciotti R., Gardini F. (2012). Effects of starter  
392 cultures and fermentation climate on the properties of two types of typical Italian dry fermented  
393 sausages produced under industrial conditions. *Food Control*, 26, 416-426

394

395 Tabanelli G., Montanari C., Grazia L., Lanciotti R., Gardini F. (2013). Effect of aw at packaging  
396 time and atmosphere composition on aroma profile, biogenic amine content and microbiological  
397 features of dry fermented sausage. *Meat Science*, 94, 177-186.

398

399 Toldrá F. (2006). Meat fermentation In Y. H. Hui, E. Castell-Perez, L. M. Cunha, I. Guerrero-  
400 Lagarreta, H. H. Liang, Y. M. Lo, D. L. Marshall, W. K. Nip, F. Shahidi, F. Sherkat, R. J. Winger,  
401 & K. L. Yam (Eds.), *Handbook of food science, technology and engineering*, Florida, USA: CRC  
402 Press.

403

404 Toldrá F., Nip W. K., Hui Y. H. (2007). Dry-fermented sausages: An overview. In F. Toldrá (Ed.),  
405 *Handbook of fermented meat and poultry*. Iowa, USA: Blackwell Publishing.

406

407 Trujillo, F.J., Wiangkaew, C., Tuan Pham, Q. (2007). Drying modeling and water diffusivity in beef  
408 meat. *Journal of Food Engineering*, 78, 74-85.

409

410 Unal B.S., Erdođdu F., Ekiz H.I., Ozdemir Y. (2004). Experimental theory, fundamentals and  
411 mathematical evaluation of phosphate diffusion in meats. *Journal of Food Engineering*, 65, 263–  
412 272.

413

414 Verboven P., Flick D., Nicolai B.M. Alvarez G. (2006). Modelling transport phenomena in  
415 refrigerated food bulks, packages and stacks: basics and advances *International Journal of*  
416 *Refrigeration*, 29, 985-997.

417

418 Wang L., Sun D.W. 2003. Recent developments in numerical modelling of heating and cooling  
419 processes in the food industry e a review. *Trends in Food Science & Technology*, 14,408-423.

420

421 Xia B., Sun D.W. (2002). Applications of computational fluid dynamics (CFD) in the food industry:  
422 a review. *Computers and Electronics in Agriculture*, 34, 5-24.

423

424 Zanardi E., Ghidini S., Conter M., Ianieri A. (2010). Mineral composition of Italian salami and  
425 effect of NaCl partial replacement on compositional, physico-chemical and sensory parameters.  
426 *Meat Science* , 86, 742–747.

427

428 Zeuthen P. (1995). Historical aspects of meat fermentations. In G. Campbell-Platt, & P. E. Cook  
429 (Eds.), *Fermented meats*. Glasgow, UK: Blackie Academic & Professional.

430

431 \*\*\*

432

### 433 **Highlights**

434 Ripening and storage stages influence the physical, chemical and microbiological transformations  
435 that take place in salami. The most important mass transport phenomenon occurring inside the  
436 matrix is the water transfer. In this work two parametric numerical models developed to study the  
437 moisture diffusion physics, during ripening and storage in package. The models were  
438 experimentally validated showing a good agreement with observed data. The models could be used  
439 to find the best conditions for ripening, packaging and distribution.

440

441 **Figure Captions**

442

443 **Figure 1:** experimental and calculated values of mean water concentration determined during 28

444 days of ripening.

445 **Figure 2:** experimental and calculated values of mean water activity determined during 28 days of

446 ripening.

447 **Figure 3:** simulated moisture concentration dry basis (a), moisture content (a) and water activity (b)

448 inside of salami after 28 days of ripening.

449 **Figure 4:** final water concentrations (28 days of ripening) as function of radius dimensions and

450 position inside of salami.

451 **Figure 5:** mean moisture contents on dry basis as function of relative humidity (75, 80 and 85%)

452 and days of ripening.

453 **Figure 6:** moisture content as function of days of storage and position inside of salami.

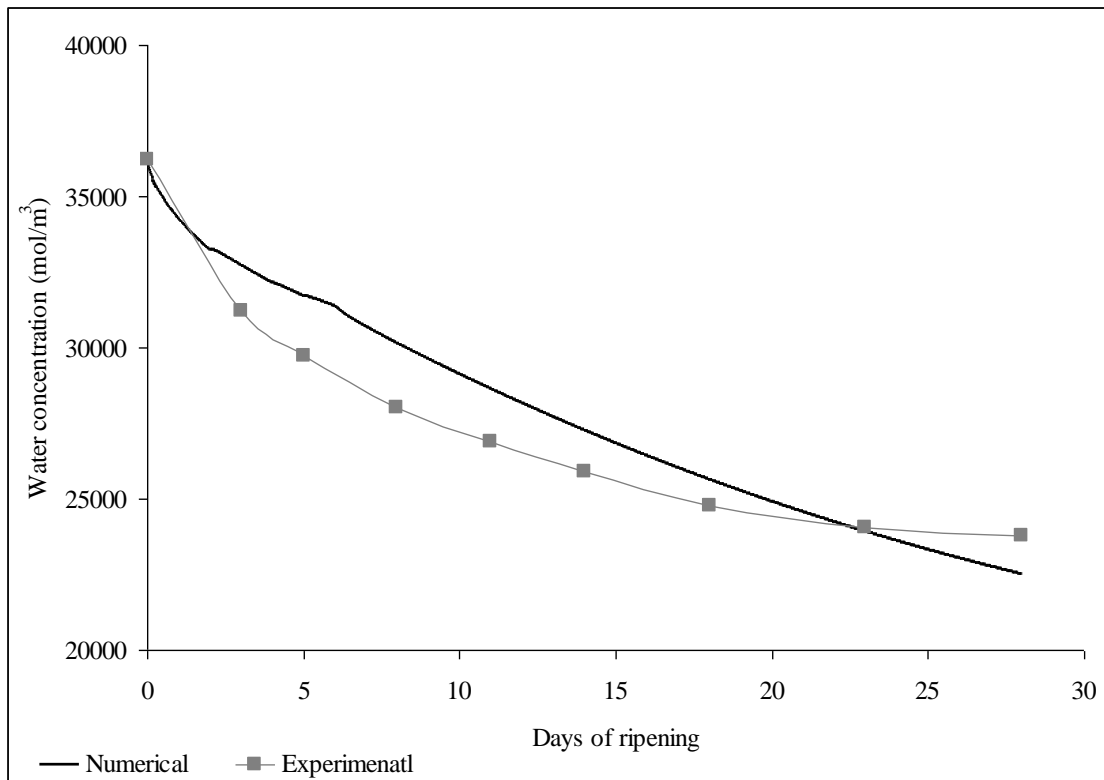
454 **Figure 7:** Mass of water in air (headspace), inside of salami and liquid (available for evaporation

455 and condensation) during storage.

456 **Figure 8:** Effect of evaporation and condensation on moisture content inside of salami.

457

458



459

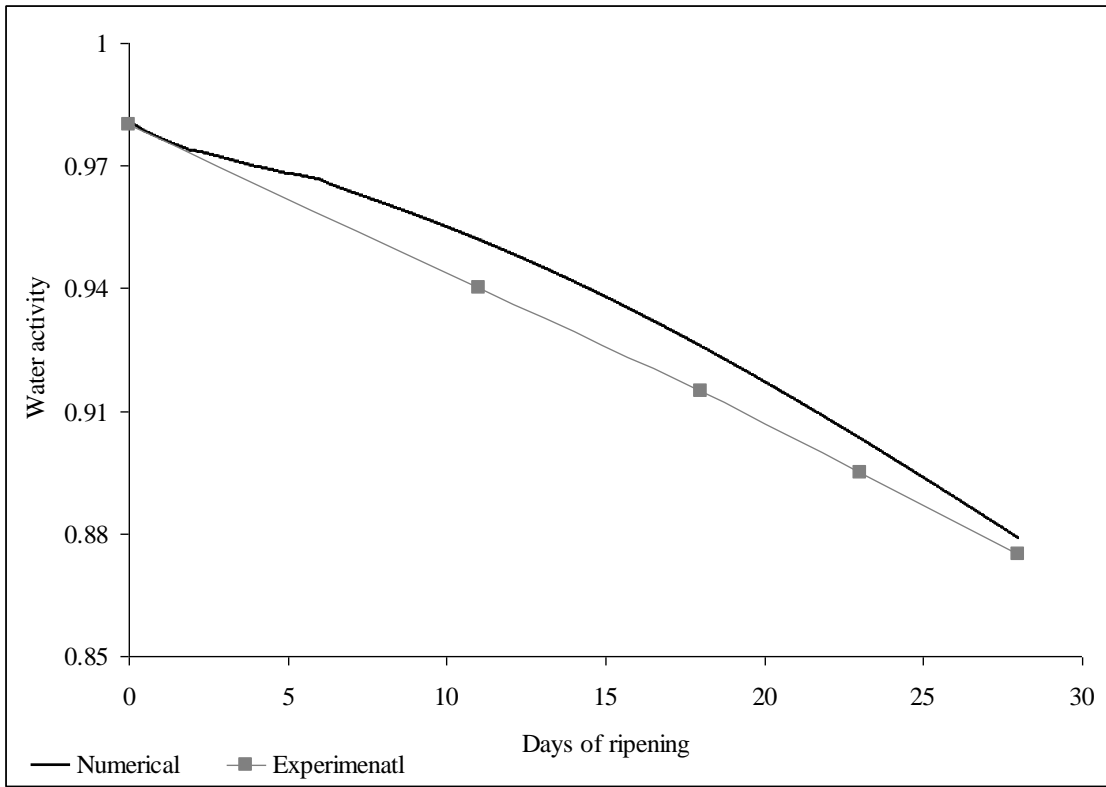
460

461

462

463

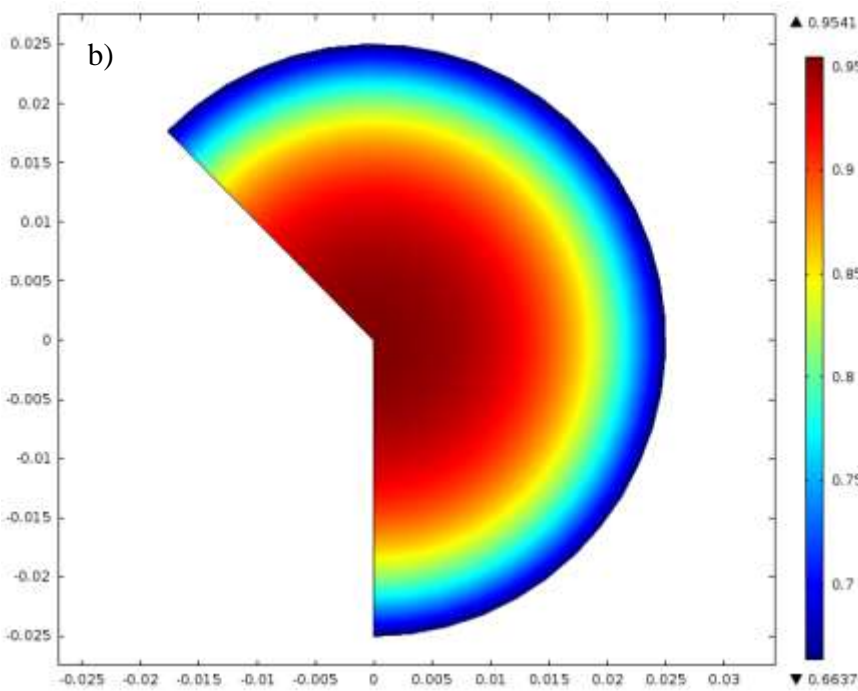
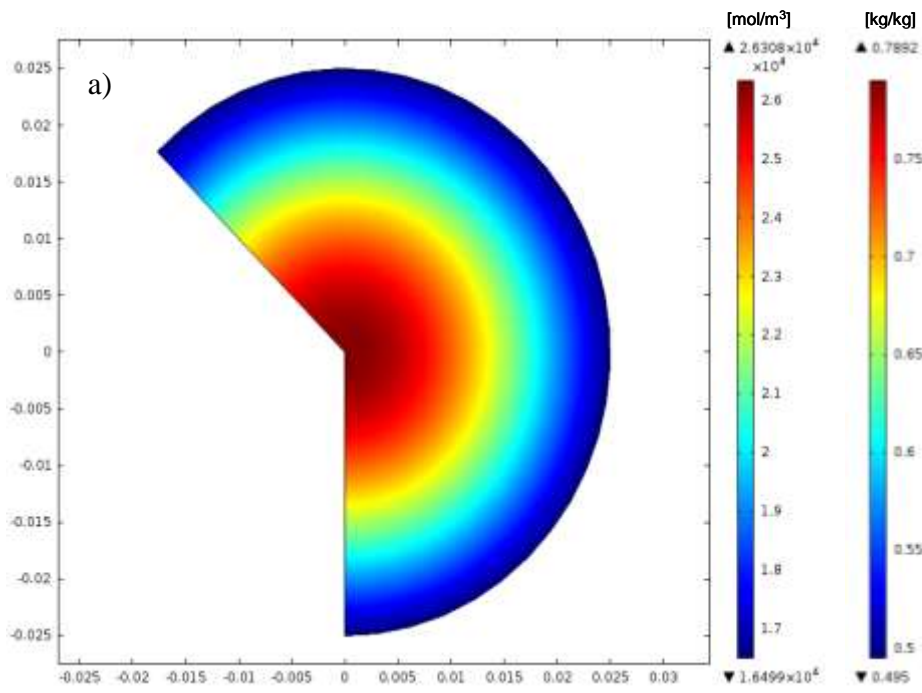
Fig1



464  
465  
466  
467  
468

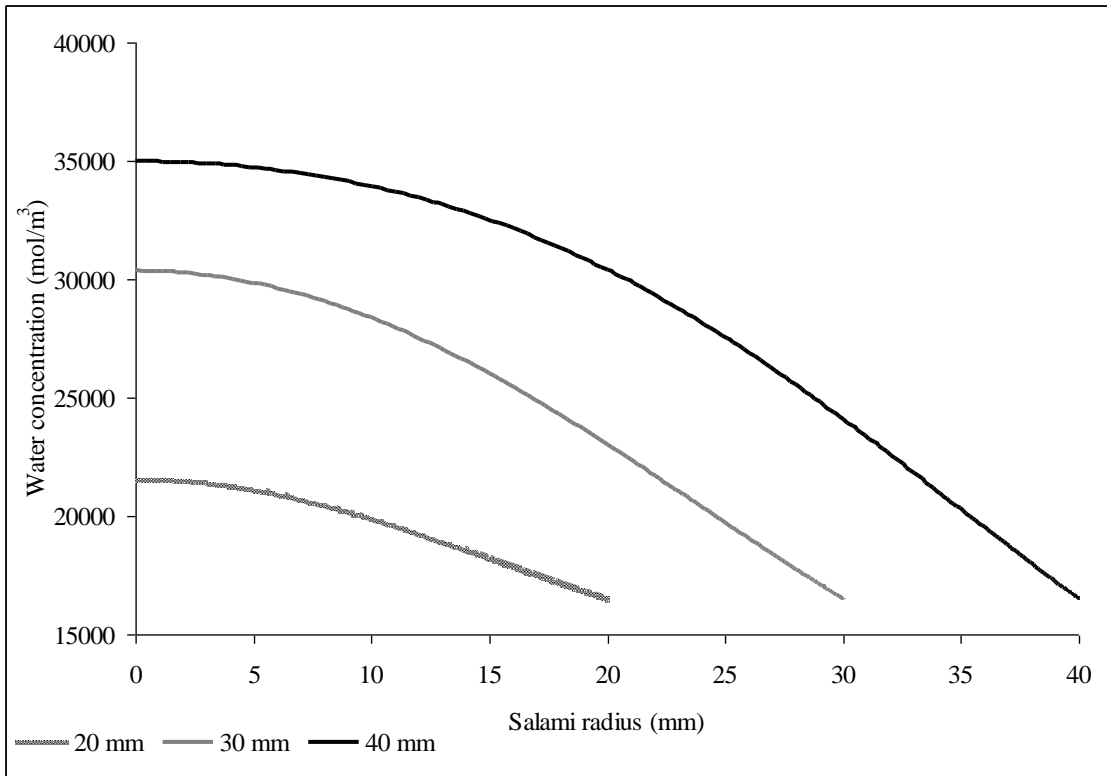
Fig 2





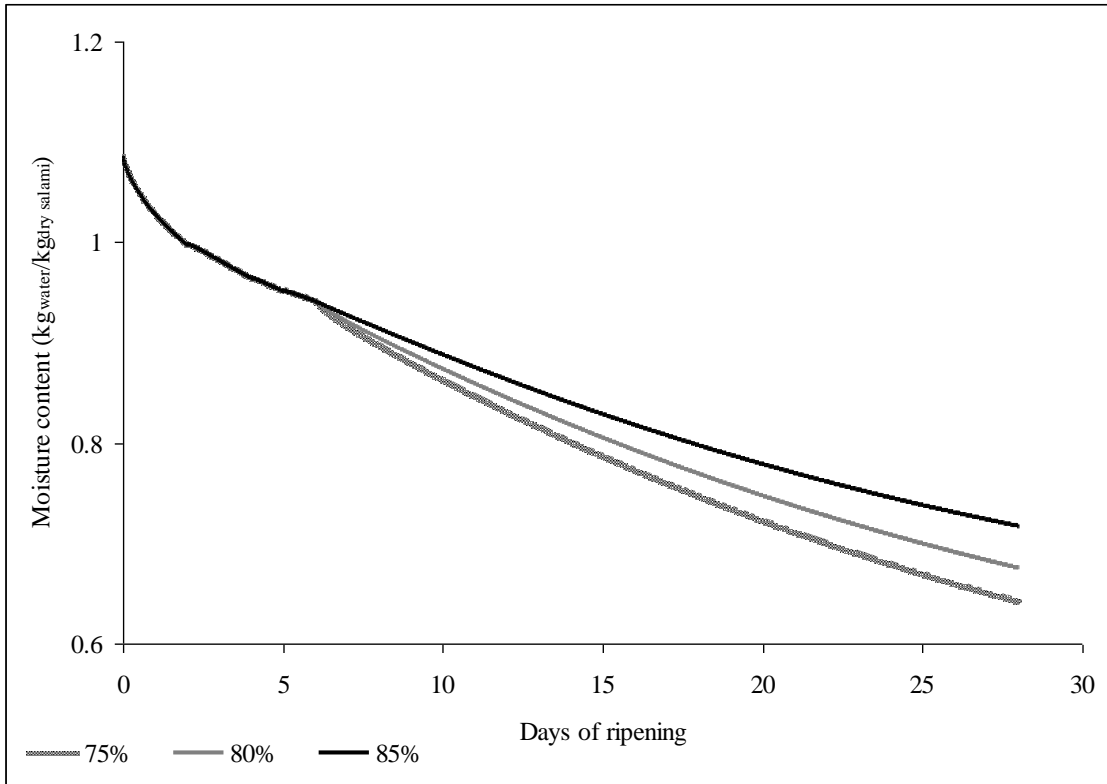
469  
470  
471  
472  
473

Fig 3



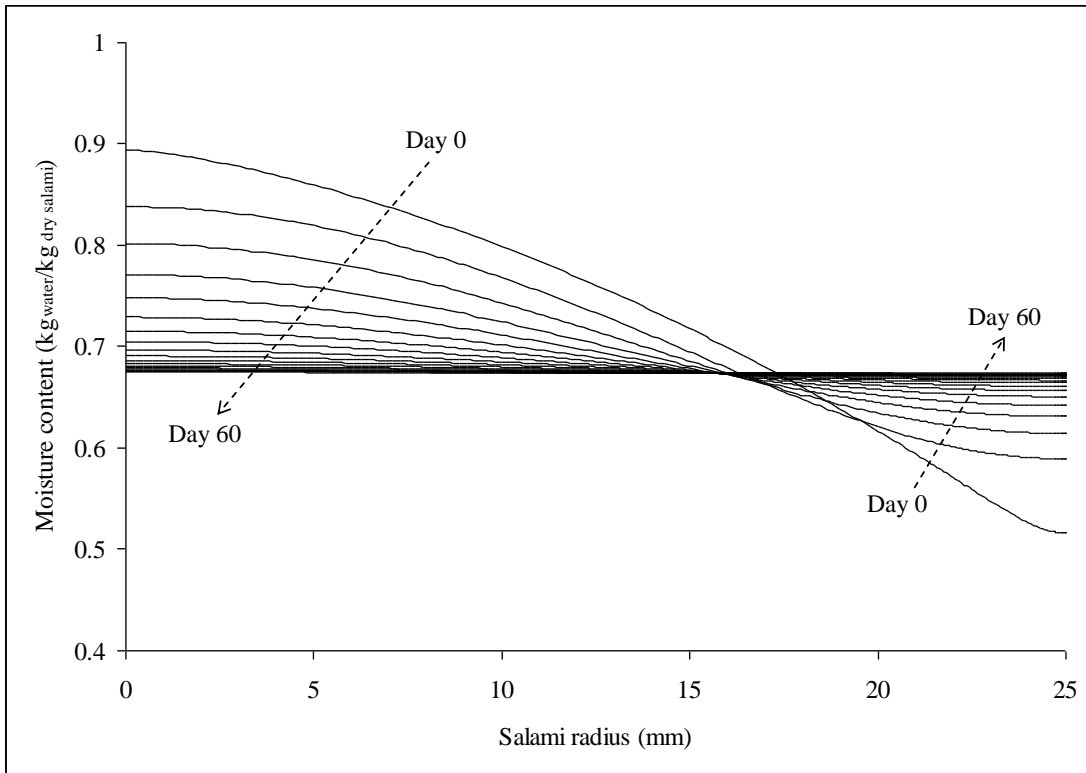
474  
475  
476  
477  
478

Fig 4



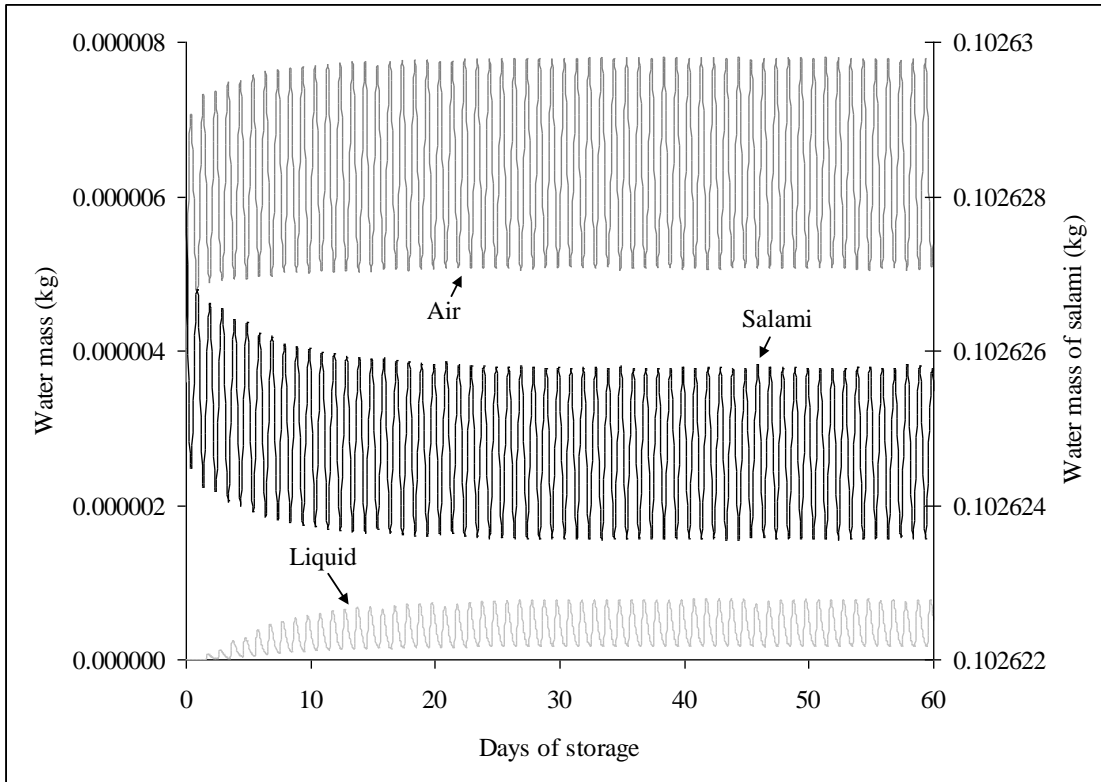
479  
480  
481  
482  
483

Fig 5



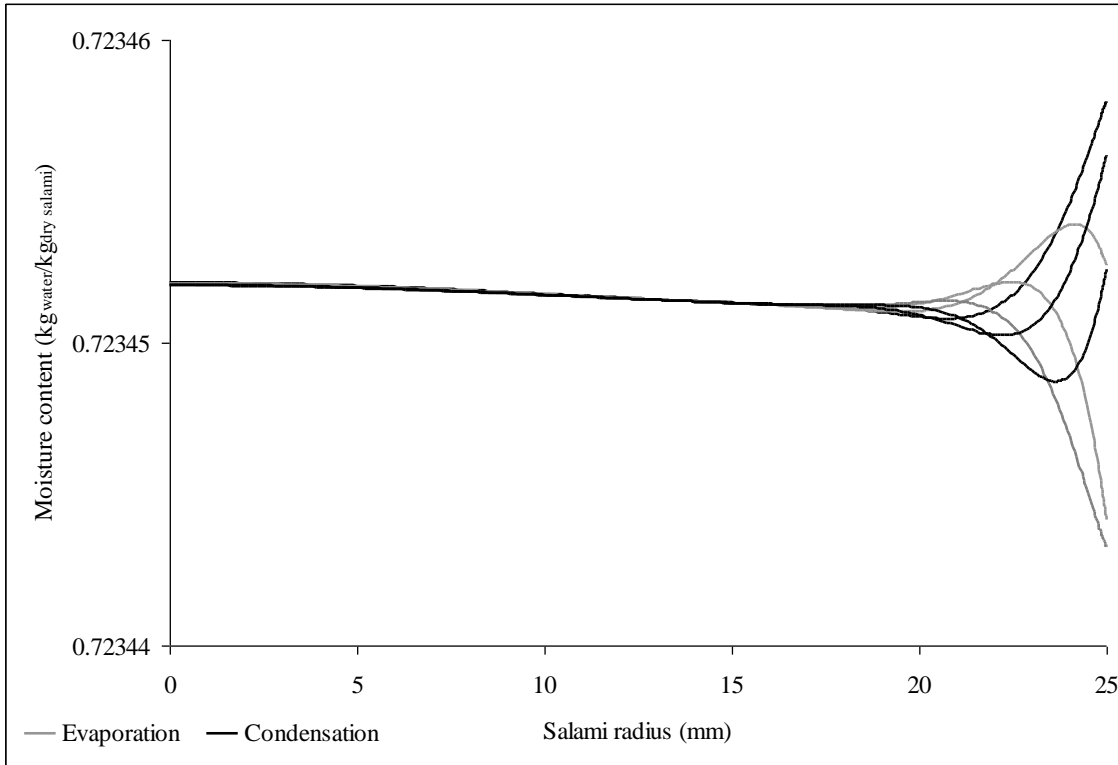
484  
485  
486  
487  
488

Fig 6



489  
490  
491  
492  
493

Fig 7



495

496

497 Fig 8

498

499

500

501

\*\*\*

502 *This paper is an Author's post-print on open access repository after an embargo period of between*503 *12 months and 48 months, released with a Creative Commons Attribution Non-Commercial No*504 *Derivatives License: <https://creativecommons.org/licenses/by-nc-nd/3.0/>*505 *Publisher DOI: <https://doi.org/10.1016/j.jfoodeng.2014.02.003>*

506

\*\*\*

507